

# Cosmic rays measurements around the knee of the primary spectrum

Andrea Chiavassa<sup>1,a</sup>

<sup>1</sup>*Dipartimento di Fisica Università degli Studi di Torino and INFN, Via P. Giuria 1, 10125, Torino (Italy)*

**Abstract.** In this contribution I will summarize and discuss some recent results about the study of the knee of the cosmic rays energy spectrum, indicating that this spectral feature is originated by astrophysical processes. I will then discuss the current experimental efforts that are giving further insights. Latest all particle spectrum measurements have shown that, between  $10^{16}eV$  and  $10^{18}eV$ , the spectrum cannot be described by a single slope power law: an hardening around  $10^{16}eV$  and a steepening around  $10^{17}eV$  have been observed. This last feature has been attributed, by the KASCADE-Grande experiment, to the heavy primary component, confirming that the energy of the elemental spectra change of slope increase with the mass of the primary particle.

## 1 Introduction

The cosmic rays energetic spectrum can be described by a power law. More than fifty years ago a change of the spectral index, around  $3 - 4 \times 10^{15}eV$  was discovered by the Moscow State University experiment[1]. Since its discovery the knee was widely studied, a breakthrough was recently obtained by the EAS experiments supplying the detection of different EAS components on an event by event basis with a resolution lower than the EAS development fluctuations. Experiments like CASHA-MIA[2], EAS-TOP[3] and KASCADE[4] operated since the nineties detecting the electromagnetic (with scintillation and/or cherenkov light detectors), muonic (with scintillation and/or tracking detectors) and hadronic (with sampling calorimeters) EAS components. These experiments were followed by arrays mainly focusing in the  $10^{16} - 10^{18}eV$  energy range. Most of them are presently running and are multi-component EAS detectors: Tibet-III[5], KASCADE-Grande[6], GAMMA[7], GRAPES-3[8], TUNKA-133[9] and Ice-Top[10].

The primary cosmic rays properties that have to be measured (possibly for each event) are: the arrival direction, the energy and the mass. Only the event arrival direction can be directly determined (with the time of flight technique), all other informations must be inferred calibrating the experiments by means of full EAS simulations. These codes are based on hadronic interaction models derived extrapolating the measurements performed by accelerator experiments operating at lower energies (before LHC the maximum center of mass energy reached was  $\sim 17eV$ ) and not measuring in the forward kinematic region (the more relevant one for EAS development). The reference EAS simulation code is CORSIKA[11] that can be run using different high energy hadronic interaction models: QGSJET-II-03[12], Sibyll2.1[13] and EPOS1.99[14].

<sup>a</sup>e-mail: [achiavas@to.infn.it](mailto:achiavas@to.infn.it)

In this contribution I will first review the main results obtained by past experiments, discussing their dependence on hadronic interaction models; then I will describe the more recent experimental achievements.

## 2 Results of past experiments

The experiments that have studied the  $10^{14} - 10^{16}eV$  energy range in the last twenty years were mainly focused in the study of the primary spectrum and chemical composition, while few results were obtained about the cosmic rays anisotropies.

### 2.1 Hadronic interaction model independent results.

Around the knee cosmic rays cannot be directly measured, thus experiments detects the EAS generated in atmosphere by the interaction of the primary particles with air nuclei. For each event the total number of particles at detection level is determined both for the electromagnetic ( $N_e$ ) and muonic ( $N_\mu$ ) components, thus the  $N_e$  and  $N_\mu$  spectra were measured at different atmospheric depths. The change of slope has been observed in the spectra of all shower components, electromagnetic[15, 16], muonic[16, 17] and hadronic[18], and at different atmospheric depths. Figure 1 (taken from[19]) shows the  $N_e$  spectra measured at different atmospheric depth, we can see that the number of electrons at the knee decreases with the atmospheric depth and that the decrease rate is in agreement with the  $N_e$  absorption in atmosphere (the same is true for  $N_\mu$ ). Moreover the integral fluxes above the knee measured for different EAS components at different atmospheric depths agree inside experimental errors[17]. All these results indicate that the knee is a feature of the primary spectrum and that it is

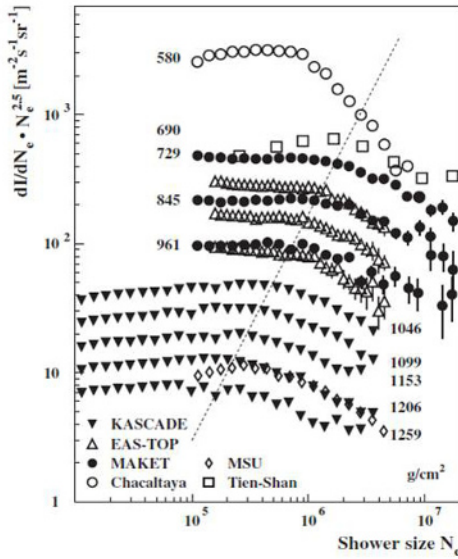


**Figure 1.** Shower size spectra measured by different experiments at different atmospheric depths. The figure is taken from[19], references to the experimental data can be found therein.

not due to a change in the hadronic interactions. The explanation of this change of slope must thus be found within astrophysical processes.

A very strong indication showing that the knee is due to the light primary component has been obtained by the KASCADE collaboration[20] measuring the muon density, at fixed distances from the shower core, spectra. Events were divided in two samples according to the ratio between the muonic and electromagnetic shower sizes calculated at a reference angle (to account for the EAS development in atmosphere), events with a large (small) value of this ratio are generated mainly by heavy (light) primaries. The result (shown in figure 2, taken from[20]) shows that the change of slope is present only in the spectrum of the "electron rich" sample, while the one of the "electron poor" events can be described by a single slope power law. This event selection is almost independent from EAS simulation, that is only used to fix the cut value (at a level corresponding to a certain primary group, e.g. the expectations for CNO). Different hadronic interaction models shift the cut value but the shapes of the "electron rich" and "electron poor" spectra remain unchanged (only the relative abundance of the two samples is modified).

The situation is less clear concerning the search for large scale anisotropies. The EAS-TOP collaboration published[21] a study of cosmic rays anisotropy using the whole data set (eight years) analyzed with the east-west method[22]. The result confirmed the amplitude of an already reported cosmic ray anisotropy[23] at  $10^{14} eV$ :  $A_{sid}^I = (2.6 \pm 0.8) \times 10^{-4}$ . Extending the analysis to higher energies (around  $4 \times 10^{14} eV$ ) a larger amplitude was found (even if the statistical significance is still limited):  $A_{sid}^I = (6.4 \pm 1.5) \times 10^{-4}$ .

The KASCADE collaboration published[24] the search for large scale anisotropy using a data set of 1600

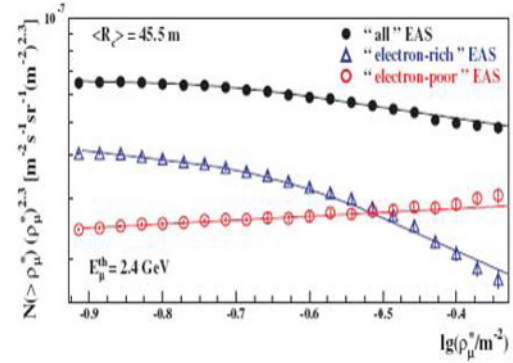


**Figure 2.** Shower size spectra measured by different experiments at different atmospheric depths. The figure is taken from[20].

days (from May 1998 to October 2002), after application of the quality cuts about 20% of the initial sample remain. The analysis is thus based on 269 sidereal days with continuous data taking. No anisotropy is reported, the derived upper fluxes limits for Rayleigh amplitudes are  $10^{-3}$  at  $7 \times 10^{14} eV$  and  $10^{-2}$  at  $6 \times 10^{15} eV$ .

## 2.2 Hadronic interaction model dependent results.

Quantitative results about the evolution of the primary chemical composition with energy can be obtained studying the two dimensional  $N_e$ ,  $N_\mu$  distributions. Results must be inferred comparing the experimental measurements with the expectations derived from EAS complete simulations. Different approaches have been used: from the simplest one comparing the mean values of  $N_\mu$  ( $N_e$ ) in bins of  $N_e$  ( $N_\mu$ ) to more sophisticated ones using the shapes of the measured distributions.

The unfolding analysis technique, introduced by the KASCADE collaboration[25], allows to obtain the differential energy spectra of single mass groups solving the integral equation:

$$N_i = 2\pi A_{eff} T \sum_{n=1}^{N_A} \int_0^{\theta_{max}} \int_{-\infty}^{+\infty} \frac{dJ_A}{d \log E} p_n \sin \theta \cos \theta d \log E d\theta \quad (1)$$

where  $N_i$  are the number of events in each pixel of the two dimensional ( $N_e$ ,  $N_\mu$ ) spectra,  $A_{eff}$  is the effective area,  $T$  is the measurement time,  $p_n$  is the conditional probability that a primary nucleus  $n$  with energy  $E$  induces a shower that is detected and reconstructed in the same ( $N_e$ ,  $N_\mu$ ) interval. This probability must be calculated from an EAS and detector complete simulation taking into account the EAS development fluctuations, the detector efficiency and the reconstruction errors.

The KASCADE collaboration[25] showed that, independently from the hadronic interaction model, the change of slope of the spectrum is observed only for light elements and that the energy of the knee increases with the mass of the primary particle. The choice of the hadronic interaction model heavily influences the absolute fluxes of the elemental spectra.

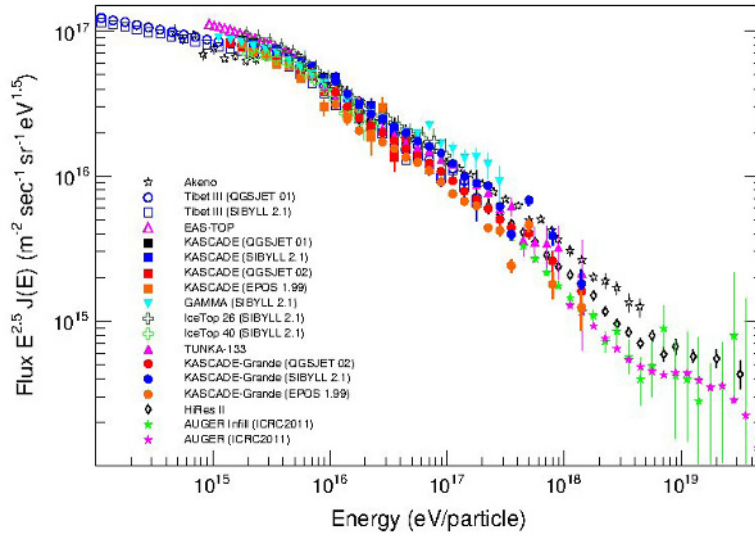


**Figure 3.** All particle spectra measured by different experiments. References to experimental data: Akeno[28], HiResII[29], TibetIII[30], Tunka-133[31], GAMMA[32], IceTop[33, 34], KASCADE[25, 35], EAS-TOP[15], KASCADE-Grande[36, 37], Pierre Auger Observatory[38, 39].

A primary chemical composition getting heavier crossing the knee energy is observed also studying the  $N_\mu$  mean values as a function of  $N_e$  by the CASA-MIA[26] experiment and fitting the  $N_\mu$  distributions in bins of  $N_e$  by the EAS-TOP[17] and the EAS-TOP+MACRO[27] collaborations.

### 2.3 Summary of past experiment results

The currently favored hypothesis about the astrophysical processes responsible for the knee involve either the limit of acceleration in galactic sources or the beginning of diffusion from local galactic magnetic fields. In both scenarios the knee of elemental spectra is expected at the same rigidity, thus the knee of the heavy components (Fe) is foreseen around  $10^{17} eV$ . This energy range cannot be studied by the experiments previously mentioned that, being too small, are facing statistical problems approaching these energies, thus bigger arrays were constructed and operate since one decade.

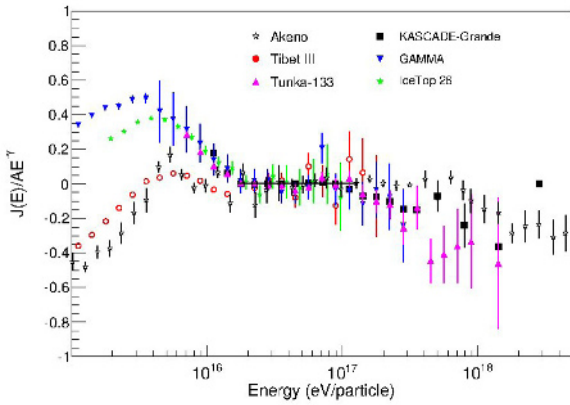
## 3 Results of current experiments

Figure 3 shows a collection of measurements of the all particle primary spectrum performed by indirect experiments operating with different detection techniques, located at different heights above sea level and calibrated by means of different hadronic interaction models. The agreement between the experiments is inside the systematic uncertainties, the differences can be mainly attributed to the choice of the hadronic interaction model, in fact comparing the results of different experiments calibrated using the same hadronic model the agreement is improved.

It is interesting to compare the shapes of these spectra, to enhance the spectral shapes a residual plot is shown in figure 4. The energy scale is based on the calibrations used by the experiments (i.e. spectra are not shifted with respect to figure 3). While the fluxes are divided by the results obtained fitting every data set with a single slope power law in the energy range between the two features claimed by KASCADE-Grande[36] (hardening at  $\sim 10^{16}$  and steepening at  $\sim 10^{17} eV$ ). We can notice as these structures are visible in all the spectra, pointing out that the primary spectrum cannot be described, in this energy range, by a single slope power law as was supposed before. These features must be further investigated, possibly relating them to the chemical composition of primary particles.

Primary chemical composition studies are approached by these experiments in different ways: the atmospheric cherenkov light detector TUNKA-133 is sensible to the atmospheric depth of shower maximum ( $X_{max}$ ), while the other arrays correlate one experimental observable related to the EAS muonic component with one sensible to the electromagnetic one:

- GRAPES-3[8]: the muon multiplicity distributions and the shower size  $N_e$ .
- IceTop-IceCube[34]:  $K_{70}$ , a parameter determined by IceCube proportional to the muon density at a slant depth of 1950 m and at 70 m distance from the shower axis, and  $S_{125}$  the particle density measured by IceTop at 125 m distance from the shower core.
- KASCADE-Grande[40]: the numbers of muons ( $N_\mu$ ) and of the total charged particle ( $N_{ch}$ ).



**Figure 4.** Residual plot of the spectra measured by different experiments with respect to a single power law fit, to the same data set, in the energy range between the spectral features claimed by the KASCADE-Grande experiment. For the references to experimental data see figure 3.

### 3.1 Energies below the knee

Below  $10^{14} eV$  a comparison between the results obtained by direct and indirect measurements can be performed. This is a very interesting point allowing a check of the indirect EAS experiments calibrations.

The ARGO-YBJ experiment[41] published the light primaries (H plus He) spectrum derived from the event multiplicity (i.e. the number of pads fired). With the event selection used in this analysis they could show (by a full monte carlo simulation) that the contribution of the CNO group primaries is lower than 2%. The measured spectrum is compared with the one directly measured, for these two primaries, by the balloon experiment CREAM[42]: the agreement found is very good.

Also the GRAPES-3 experiment operates at energies below the knee of the primary spectrum and compares the derived elemental spectra with those directly measured by the JACEE[43], RUNJOB[44] and CREAM[42] balloon detectors showing a good agreement.

Bridging the direct and indirect elemental spectra measurements is a very important achievement. In the near future these results (at least for the H and He primaries) will be extended up to the knee determining which is the dominating component and giving a reference for the experiments studying the higher energies.

### 3.2 Energies above the knee

Moving to energies above the knee current experiments confirm the previously discussed measurement of a primary chemical composition getting heavier and extend the studies above  $10^{17} eV$ .

The TUNKA-133[45] experiment measuring the behavior of the  $X_{max}$  mean values as a function of the primary energy shows that up to  $\sim 4 \times 10^{16} eV$  the trend is to move from the expectations (based on the QGSJET-II hadronic

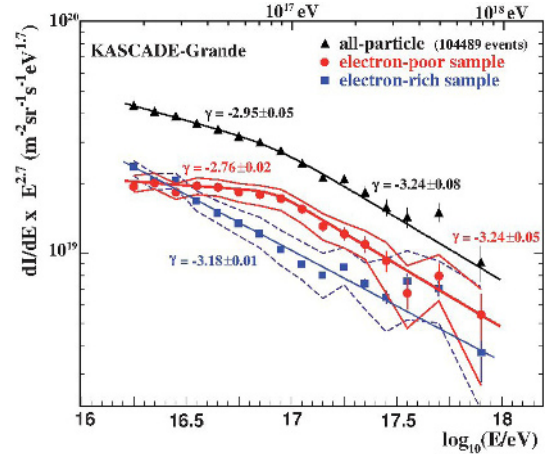


**Figure 5.** Energy spectra, measured by the KASCADE-Grande collaboration, dividing the events into the electron poor (i.e. heavy elements) and electron rich (i.e. light primaries) samples.

interaction model) for pure H primaries toward those for pure Fe, while above this energy the trend is parallel to the Fe ones.

The IceTop-IceCube[34] measurements indicate the same tendency in the covered energy range (actual results reach  $\sim 4 \times 10^{16} eV$ ), being IceCube a deep under ice detector this analysis sample a different kinematic region with respect to surface arrays. This kind of measurements were previously performed only by the EASTOP and MACRO[27] experiments, the results obtained at lower energies showed the same trend toward a composition dominated by heavier elements.

The KASCADE-Grande experiment, being located well beyond the maximum shower development and having reached an high resolution, transferred to energies above the knee the analysis techniques introduced by the KASCADE collaboration at lower energies. The two dimensional ( $N_{\mu}$ ,  $N_{ch}$ ) spectra are analyzed both with the unfolding technique and dividing, accordingly to the  $\lg N_{\mu}$ ,  $\lg N_{ch}$  ratio, the event sample in the "electron rich" and "electron poor" families, corresponding to light and heavy primaries.

The unfolding analysis[46] (based on the QGSJET-II interaction model) allows to determine the spectra of three mass groups and indicates a composition dominated by heavy (Fe) elements, whose spectrum steepens at  $\sim 8 \times 10^{16} eV$ . The intermediate (He+C+Si) and light (H) elements spectra can be described by a single power law, even if the uncertainties are huge and the result must be further investigated.

As in the case of KASCADE the analysis aiming to measure the spectra of the "electron rich" and "electron poor" event samples is less dependent on the interaction model used in the EAS simulation. Figure 5 shows the results of the KASCADE-Grande collaboration[40]. We can notice as both the all particle and the heavy primaries spectra show a kneelike feature. Applying a fit of two power

laws of the spectrum interconnected by a smooth knee[47] the following results are obtained:

- all particle spectrum. Break position  $\log E/eV = 16.92 \pm 0.10$ . The spectral slope changes from  $\gamma_1 = -2.95 \pm 0.05$  to  $\gamma_2 = -3.24 \pm 0.08$ . Statistical significance that the entire spectrum cannot be fitted by a single power law  $2.1\sigma$
- Heavy primaries. Break position  $\log E/eV = 16.92 \pm 0.04$ , spectral slopes from  $\gamma_1 = -2.76 \pm 0.02$  to  $\gamma_2 = -3.24 \pm 0.05$ . Statistical significance  $3.5\sigma$

hence the kneelike feature already observed in the all particle spectrum is enhanced in the spectrum of the heavy primaries. Shifting the cut value to separate the events into the "electron rich" and "electron poor" samples (i.e. using a different hadronic interaction model) the kneelike structure of the "electron poor" sample is retained, only the fraction of events in the two samples is modified.

### 3.3 Summary of current experiments results

Summarizing all these experimental results about single elements (or mass groups) spectra obtained in the energy range around the knee, from  $10^{13}$  to  $10^{18}eV$ , the situation may appear confused and contradictory. But most of the differences are probably due to the hadronic interaction models used in the EAS simulations to determine the primary energy.

In fact if we arbitrarily select some of the experimental results a more coherent picture of the elemental spectra can be derived. Figure 6 is a personal compilation of elemental mass groups spectra. I want to stress that in this plot results obtained by different hadronic interaction models are merged and so it is not intended as a possible description of the cosmic rays elemental spectra from  $10^{13}$  to  $10^{18}eV$ . The apparently good agreement between different measurements can be fortuitous (as different hadronic interaction models are used), nevertheless a general common trend in the shapes of the mass groups spectra is present. All spectra present a kneelike feature at an energy increasing with the mass of the primaries, as is expected by the astrophysical models describing the knee of the primary spectrum.

## 4 Conclusions and Perspectives

Recent achievements about the knee of the primary cosmic rays spectrum can be thus summarized:

- the knee is observed in the spectra off all EAS components.
- The integral fluxes above such features are consistent.
- The knee can be attributed to the light component of cosmic rays.
- A kneelike feature has been detected, around  $8 \times 10^{16}eV$  in the spectrum of the heavy component.
- The all particle spectrum between  $10^{16}$  and  $10^{18}eV$  cannot be described by a single power law.

Important additional informations are expected in the near future and will highly contribute to clarify the situation:

- elemental spectra of H and He primaries up to the knee.
- Primary anisotropies measurements above  $\sim 5 \times 10^{15}eV$ .
- Finally EAS simulation codes will be highly improved using the measurements of the LHC experiments.

## References

- [1] G. Kulikov and G. Khristiansen, *Sov. Phys. JETP* **8**, 441 (1959).
- [2] Borione A. et al., *Nucl. Instr. & Meth. A* **346**, 682 (2000).
- [3] M. Aglietta et al., *Nucl. Instr. & Meth. A* **336**, 310 (1993).
- [4] T. Antoni et al., *Nucl. Instr. & Meth. A* **513**, 490 (2003).
- [5] M. Amenomori et al., *Astrophys. J.* **461**, 408 (1996).
- [6] W.D. Apel et al., *Nucl. Instr. & Meth. A* **620**, 202 (2010).
- [7] A.P. Garyaka et al., *J. Phys. G: Nucl. Part. Phys.* **35**, 115201 (2008).
- [8] H. Tanaka et al. *J. Phys. G: Nucl. Phys.* **39**, 025201 (2012).
- [9] S.F. Berezhnev et al., *Nucl. Instr. and Meth. A* **692**, 98 (2012).
- [10] R.U. Abbasi et al., arXiv:1207.3455v1 (2012).
- [11] D. Heck et al., Report FZKA 6019, Forschungszentrum Karlsruhe (Germany), (1998).
- [12] S. Ostapchenko, *Nucl. Phys. B (Proc. Suppl.)* **151**, 143 (2006)
- [13] E.-J. Ahn et al., *Phys. Rev. D* **80**, 094003 (2009).
- [14] K. Werner. *Nucl. Phys. B (Proc. Suppl.)* **175**, 81 (2008).
- [15] M. Aglietta et al., *Astropart. Phys.* **10**, 1 (1999).
- [16] R. Glasstetter et al., *Proc. 26th Int. Cosmic Ray Conf. (Salt Lake City)* **1**, 222 (1999).
- [17] M. Aglietta et al., *Astropart. Phys.* **21**, 583 (2004).
- [18] J. Hörandel et al., *Proc. 26th Int. Cosmic Ray Conf. (Salt Lake City)* **1**, 337 (1999).
- [19] A. Haungs, H. Rebel & M. Roth, *Rep. Prog. Phys.* **66**, 1145 (2003).
- [20] T. Antoni et al., *Astropart. Phys.* **16**, 373 (2002).
- [21] M. Aglietta et al., *Astrophys. J.* **692**, L130 (2009).
- [22] R. Bonino et al., *Astrophys. J.* **738**, 67 (2011).
- [23] M. Aglietta et al., *Astrophys. J.* **470**, 501 (1996).
- [24] T. Antoni et al., *Astrophys. J.* **604**, 687 (2004).
- [25] T. Antoni et al., *Astropart. Phys.* **24**, 1 (2005).
- [26] M.A.K. Glasmacher et al., *Astropart. Phys.* **12**, 1 (1999).
- [27] M. Aglietta et al., *Astropart. Phys.* **21**, 223 (2004).
- [28] M. Nagano et al, *J.Phys.G* **10**, 1295 (1984). M. Nagano et al., *J.Phys.G* **18**, 423 (1992).
- [29] R.U. Abbasi et al., *Phys. Rev. Lett.* **100**, 101101 (2008).

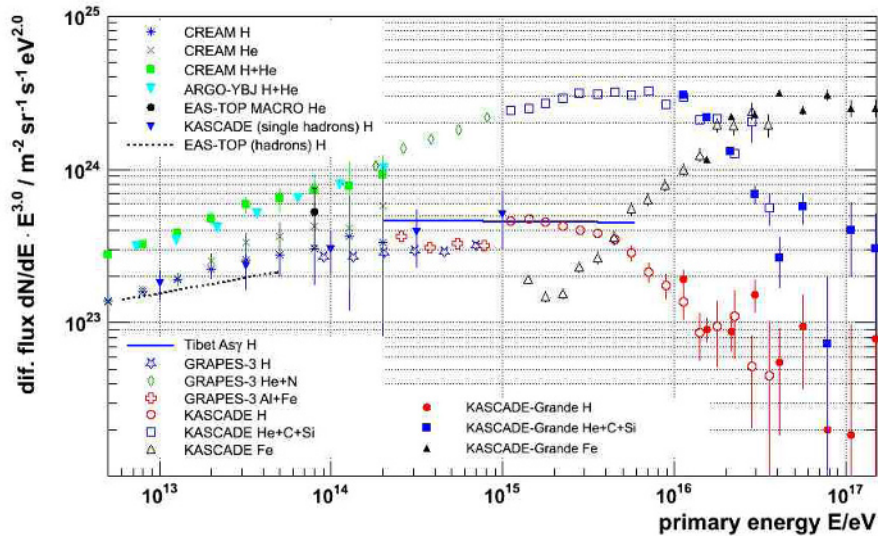


**Figure 6.** Compilation of arbitrarily selected sample of primary cosmic rays elemental spectra. The agreement between the absolute fluxes may be fortuitous as they are derived by different hadronic interaction models, while the one between their shapes is, in my opinion, more relevant. References to experimental data: CREAM[42], ARGO-YBJ[41], EAS-TOP+MACRO[27], KASCADE[35, 48], EAS-TOP[49], TibetASy[50], GRAPES-3[8], KASCADE-Grande[46].

- [30] M. Amenomori et al., *Astrophys. J.* **678**, 1165 (2008).
- [31] L. Kuzmichev et al., *Proc. 32nd Int. Cosmic Ray Conf. (Beijing)* **1**, 209 (2011).
- [32] R. Martirosov et al., *Proc. 32nd Int. Cosmic Ray Conf. (Beijing)* **1**, 178 (2011).
- [33] R.U. Abbasi et al., arXiv:1202.3039v1 (2012).
- [34] R.U. Abbasi et al., arXiv:1207.3455v1 (2012).
- [35] M. Finger PhD Thesis, Karlsruhe Institut für Technology (2011), <http://d-nb.info/1014279917/34>
- [36] W.D. Apel et al., *Astropart. Phys.* **36**, 183 (2012).
- [37] W.D. Apel et al., Submitted to *Advances in Space Research, COSPAR 2012 (Mysore)*, (2012).
- [38] J. Maris et al., *Proc. 32nd Int. Cosmic Ray Conf. (Beijing)* **1**, 267 (2011).
- [39] F. Salamida et al., *Proc. 32nd Int. Cosmic Ray Conf. (Beijing)* **2**, 145 (2011).
- [40] W.D. Apel et al., *Phys. Rev. Lett.* **107**, 171104 (2011).
- [41] B. Bartoli et al., *Phys. Rev. D* **85**, 092005 (2012).
- [42] Y.S. Yoon et al., *Astrophys. J.* **728**, 122 (2011).
- [43] K. Asakimori et al., *Astrophys. J.* **502**, 278 (1998).
- [44] V.A. Derbina et al., *Astrophys. J.* **628**, L41 (2005).
- [45] V. Prosin et al., *Proc. 32nd Int. Cosmic Ray Conf. (Beijing)* **1**, 197 (2011).
- [46] D. Fuhrmann et al., *Proc. 32nd Int. Cosmic Ray Conf. (Beijing)* **1**, 227 (2011).
- [47] T. Antoni et al., *Astropart. Phys.* **16**, 245 (2002).
- [48] T. Antoni et al., *Astrophys. J.* **612**, 914 (2004).
- [49] M. Aglietta et al., *Astropart. Phys.* **19**, 329 (2003).
- [50] M. Amenomori et al., *Physics Letters B* **632**, 58 (2006).